Variability of Tropospheric carbon monoxide and ozone over India using IASI/MetOp sounder and aircraft (MOZAIC) with the simulations of MOZART-4

Y. Yarragunta[a, b], S. Srivastava[a], D. Mitra[a] and H.C. Chandola[b]

[a]*Marine & Atmospheric Sciences Department, Indian Institute of Remote Sensing, Dehradun-248001*
[b]*Department of Physics, D.S.B. Campus, Kumaun University, Nainital-263001*

ABSTRACT

In the present study, tropospheric ozone (O_3) and carbon monoxide (CO) have been simulated using MOZART-4 (Model for Ozone and Related chemical Tracers-Version4) during 2007-08. The model simulated O_3 and CO are evaluated against the IASI (Infrared Atmospheric Sounding Interferometer) observations and MOZAIC (Measurement of Ozone and Water Vapor by Airbus In-Service Aircraft) measurements. The modeled vertical distributions of O_3 and CO agree well with the MOZAIC observations over central Indian site, Hyderabad. The mean of the simulated O_3 mixing ratio is 51±10 ppbv for LT (lower troposphere) while 57±12 ppbv for MT (middle troposphere). The corresponding observed O_3 mixing ratio is 43±15 ppbv and 49±15 ppbv respectively. The mean of the simulated CO mixing ratio is 137±54 ppbv for LT while 96±20 ppbv for MT. whereas the corresponding observed CO mixing ratio is 151±60 ppbv and 109±25 ppbv respectively. Results show good agreement between the modeled and observed mixing ratios of O_3 and CO with correlation coefficient of 0.69 and 0.80 respectively in the LT whereas 0.60 and 0.39 in MT respectively. The simulated O_3 and CO mixing ratio show good agreement with IASI observations.

Key wards: Ozone, Carbon monoxide, MOZART-4, vertical distribution and tropospheric column.

1. Introduction

Tropospheric O_3 is estimated as third most important anthropogenic greenhouse gas (Ramaswamy et al., 2001) and plays a crucial role in the earth's radiation budget (Gauss, 2003). Elevated levels of O_3 in the atmospheric boundary layer may badly affect human health and vegetation (Adams et.al., 1989). O3 plays a crucial role in atmospheric chemistry through initiation of photochemical oxidation process via direct reaction, photolysis and the subsequent reactions of photoproducts to form hydroxyl (OH) radical (Monks, 2005). It is produced in the troposphere by photochemical reactions of CO and VOCs with OH radical in the presence of NOx and sunlight. Apart from this, downward transport of stratospheric O3 into the troposphere is another source of the tropospheric O_3. The contribution of later is much smaller on an annual and global scale, but it can be accountable in the regions of subsidence (Cooper et al., 2002). Anthropogenic activities (such as combustion of biofuel and fossil fuel), biomass burning, biogenic sources and lighting are the major sources to release O_3 precursor gasses (such as CO, Nitrogen oxides (NOx) and volatile organic compounds (VOCs), etc.) in the atmosphere. During latest half of the 20th century, the fast economic growth and rapid industrialization of the developing countries has led to a dramatic increase in emissions of the O3 precursors in the atmosphere. This subsequently lead to increase in ozone concentration in the lower troposphere (Wang et al., 2006;Roy et. al., 2008; Kim et al., 2013).

CO has serious health effects on humans at higher levels in the boundary layer (Ukpebor et al., 2010). It play an important role in the atmospheric chemistry by destroying OH radical which determines the oxidizing capacity of atmosphere. The removal of CO is largely (~90%) determined by the reaction with OH radical and remaining (~10%) by soils. It is important in the climate change context, as it indirectly controls the radiative forcing by affecting concentrations of greenhouse gasses like O3 and methane (CH_4) (Wigley et al., 2002). Primarily, CO produced by biomass burning and fossil fuel combustion accounts for approximately half of global CO production in the troposphere. Another half of CO is originated from the photochemical reactions of CH_4 and non-methane hydrocarbons (NMHC), like isoprene. CO is used as tracer for the anthropogenic pollution (Jaffe et al., 1997; Wang, 2002) as well as for validating chemistry transport models (Kiley et al., 2002;Tan et al., 2004;Yarragunta et al., 2017) due to its mean tropospheric lifetime of 2-3 months (*Xiao et al.*, 2007;*Yashiro et al.*, 2009). Various emission inventories have been developed to account the contribution of major sources of CO (Granier et al., 2011). The man-made emission estimates among these inventories range from 500 to 600 Tg/yr in 2000, with negative global trend of 4% as estimated by the Monitoring Atmospheric Composition and Climate CityZen (MACCity) inventory for the period of 2000-10 (Granier et al., 2011). Most of the emission inventories have estimated an increasing trend in the regional budget of CO for China and India due to rapid industrialization and urbanization (Granier et al., 2011; Ohara et al., 2007). Anthropogenic emissions increased over Asia particularly over Indian region by 50 Tg/yr to 80 Tg/yr during period 1998-2010 (Granier et al., 2011).

Therefore, it is important to understand the spatial and temporal distribution of these gases and the contribution of various emission sources to their budget in the atmosphere. Chemistry transport modelling is a

very useful tool to quantify the amount of contribution coming from different sources and processes (chemistry, transport). In situ measurements of vertical distribution of ozone and related trace gases and their evaluation with model simulations are very limited over the Indian region (Kumar et al., 2012). In the present work, MOZART-4 (Model for OZone and related Chemical Tracers Version -4), a global chemistry transport model, has been validated over the Indian subcontinent. O_3 and CO mixing ratios obtained from satellite observation (IASI) and in situ observations (MOZAIC -http://mozaic.aero.obs- mip.fr) have been used to understand the variability of these gases over the Indian subcontinent and to validate the chemistry transport model MOZART.

2. Model and Observational Data Description

2.1 The MOZART-4 Model

The Model for Ozone and Related chemical Tracers-Version-4 (MOZART-4) is a global chemistry transport model which is developed jointly by the National Center for Atmospheric Research (NCAR), the NOAA Geophysical Fluid Dynamics Laboratory (GFDL) and the Max Planck Institute for Meteorology (MPI-Met). MOZART-4 was run with comprehensive tropospheric chemistry, includes chemical mechanism of 85 gas-phase species, 12 bulk aerosol compounds, 39 photolysis and 157 gas phase reactions (*Emmons et al.*, 2010). This offline chemical transport model is driven by meteorological fields from the National Centers for Environmental Prediction/Global Forecast System (NCEP/ GFS) for the time period of 2007-2008. The model outputs are saved daily form 01 July 2006 to 31 December 2008 and first 6 months of simulated data has been considered as spin up time (01 July 2006 – 31 December 2006). The horizontal resolution has 2.8^0 latitude by 2.8^0 longitude with 28 sigma pressure levels starting from the surface up to about 2.7 hPa.

2.2 IASI O_3 and CO observations

The MetOp polar-orbiting satellites, MetOp-A and B were launched successfully in 2006 and 2012 respectively. Each carry an IASI (Infrared Atmospheric Sounding Interferometer) instrument which possess a nadir viewing Fourier transform spectrometer observing the Earth-atmosphere in the 645-2760 cm−1 band of thermal infrared radiation (TIR) (Clerbaux et al., 2009) with a resolution of 0.5 cm−1 after apodization. IASI provides global Earth coverage twice a day, with an overpass time at ~9.30 and ~21.30 local time. At nadir, spatial resolution is 50×50 km and consists of an array of 2×2 individual circular pixels each characterized by a 12 km footprint. It is designed primarily to retrieve atmospheric humidity and temperature in order to improve weather forecasting. This also determines the global concentrations of atmospheric trace gases such as O_3 (Eremenko et al., 2008; Boynard et al., 2009) and CO (George et al., 2009) due to its large spatial coverage, high radio-metric resolution and accuracy.

2.3 IAGOS O_3 and CO observations

The MOZAIC project was initiated in the year 1993 with the aim to provide continuous and automated measurements of vertical atmospheric profiles of CO and O_3 along with observations of meteorological parameters such as temperature, pressure, wind, relative humidity and water vapor mixing ratio from aircraft A340 (Marenco et al., 1998). The MOZAIC program currently known as the European In-service Aircraft for a Global Observing System (IAGOS) program (Nedelec et al., 2015). The Gas Filter Correlation technique was used for the CO measurements using Thermo Environmental Instrument (Model 48CTL). The absorption of infrared radiation at a wavelength of 4.67 μm was used for detection of CO. The CO measurements are available at 300m vertical resolution with measurement precision of ±5 ppbv (signal noise), ± 5% (calibration) and minimum detection limit of 10 ppbv. A dual-beam ultraviolet absorption instrument from Thermo-Electron (Model 49-103) is used for the O_3 measurement and having a detection limit of 2 ppbv. Thouret et al.,(1998). and Nedelec et al., (2003) have provided additional description about measurement techniques, instrument calibration, validation and instrument quality testing for O_3 and CO respectively. For the present study, we have used IAGOS profiles measured at take-off and landing near Hyderabad in central India for 2007-08. For both gases, we could use 8-18 profiles for each season.

2.4. Methodology

The direct comparison of simulated trace gas amounts with satellite retrievals are not possible. This is because a trace gas retrieval by satellite depends on the relative sensitivity of the retrieval to different altitudes in the atmosphere and on the a priori information of retrieved trace gas profile. The averaging kernel and a priori profile associated with each IASI retrieval must be applied to the model profiles, as described in Emmons et al. (2010). The model simulated profiles are first linearly interpolated on the 43 vertical retrieval levels of IASI geographical grids. Then, the averaging kernels associated with each IASI measurement and its a priori profile are applied to the interpolated modeled profile. The comparisons are made for daily averaged profiles on the 1^0x1^0 IASI grid. To accomplish this, classical smoothing equation (1) is applied on MOZART O_3 and CO profiles (Deeter, 2013).

$$x_{ret} = x_a + A_{IASI}(x_{MOZ} - x_a) \qquad \text{Eq. (1)}$$

where x_{ret} is corresponds to retrieved or comparison profile, x_a represents the IASI a priori profile, A_{IASI} represents the IASI averaging kernel matrix and x_{MOZ} represents the raw MOZART model profile.

3. Results and Discussions

3.1 Comparison with IAGOS measurements

Hyderabad (17°27′N, 78°28′E) is located in the southern peninsular state of Telangana in India which is the fourth largest city of India. Hyderabad is situated at the altitude of 545m above the mean sea level and its urban/metropolitan inhabitants according to Census 2011 is 7.6 million spread over an area of 625 km^2. The total rainfall amount of ~700 mm occurring mostly during the monsoon season. The vertical distribution of MOZAIC and model simulated O_3 and CO have been compared in the following section in order to know the ability of model on vertical distribution of these gases.

3.1.1 Vertical Distributions of O_3 and CO

Over Hyderabad, more than 100 MOZAIC aircraft vertical profiles in each case of CO and O_3 have been analysed during 2007-08. Profiles have measurements between pressure levels 980 - 220 hPa, usually up to about 300 hPa (200 hPa) with regard to the ascent (descent) profile. We have considered only descent profiles due to availability of more profiles during the study period. The collocated profiles from the model is extracted over the grid box nearest to the MOZAIC airport. We confined to analyse these profiles from 900 hPa to 300 hPa only which provides maximum content of tropospheric information and minimum information about the stratospheric contamination. We have calculated seasonal mean of available O_3 and CO profiles. The seasons considered in the present study are, DJF (Dec-Feb), MAM (March-May), JJA (June - Aug) and SON (Sep - Nov).The model-simulated vertical distribution of O_3 and CO mixing ratios and corresponding MOZAIC/IAGOS observations over Hyderabad have been compared in the following section.

Fig. 1(a) and (b) shows the average vertical distributions of O_3 and CO with ±1σ variation along with their absolute difference (model simulated minus observed). It can be seen that the seasonal variability of vertical distribution of O_3 and CO have been reproduced by the model reasonably well in the troposphere. The model simulated and observed ozone mixing ratio increase towards higher altitude except in winter season. The column average simulated ozone mixing ratio is 56 ± 7 ppbv, 62 ± 9 ppbv, 44 ± 7 ppbv and 55 ± 10 ppbv for DJF(winter), MAM (pre-monsoon) JJA (monsoon) and SON (post-monsoon) respectively and their corresponding observed ozone mixing ratio is 49 ± 11 ppbv, 56 ± 13 ppbv, 35 ± 11 ppbv and 46 ± 15 ppbv respectively. The simulated and measured O_3 mixing ratio are found to be high during MAM and low during JJA. The variability (1σ percentage) of simulated O_3 mixing ratio is 11-19 %, 13-17 %, 13-15 % and 13-16 % during DJF, MAM, JJA and SON respectively while observed O_3 variability is 11-23 %, 10-17 %, 12-21% and 12-17% respectively. This represents the seasonality in ozone variability is consistent in the troposphere. The vertical variation of O_3 mixing ratio, shows that, simulated ozone mixing ratio is maximum during pre-monsoon season and minimum during monsoon season which is similar to observed mixing ratio except very low concentrations during monsoon season. The low concentrations during monsoon season is attributed to cloudy-rainy conditions and wind direction. This south-westerly wind during monsoon brings moist air from the Indian Ocean and Bay of Bengal.

The model simulated and observed CO mixing ratio is decreasing from 900 hPa towards 300 hPa in all four seasons. The average simulated CO mixing ratio is 150 ± 22 ppbv, 120 ± 25 ppbv, 99 ± 14 ppbv and 148 ± 31 ppbv for DJF, MAM JJA and SON respectively and their corresponding observed CO mixing ratio is 134 ± 24 ppbv, 132 ± 24 ppbv, 98 ± 15 ppbv and 117 ± 25 ppbv respectively. The high simulated CO mixing ratio has been found during DJF and SON while high measured CO has been found during DJF and MAM. The variability (1σ percentage) of simulated CO mixing ratio is 8-27 %, 6-24 %, 11-19 % and 7-27 % during DJF. MAM, JJA and SON respectively while observed CO variability is 7-30 %, 6-23 %, 9-23% and 8-28% respectively. The significant difference of observed and simulated CO mixing ratio is seen throughout the troposphere. The simulated and observed CO shows the pollution impact in lower troposphere upto 700 hPa during DJF and SON. The high concentrations during DJF and SON are attributed to heavy biomass burning from forest fires and crop residue burning (Venkataraman et al., 2006).

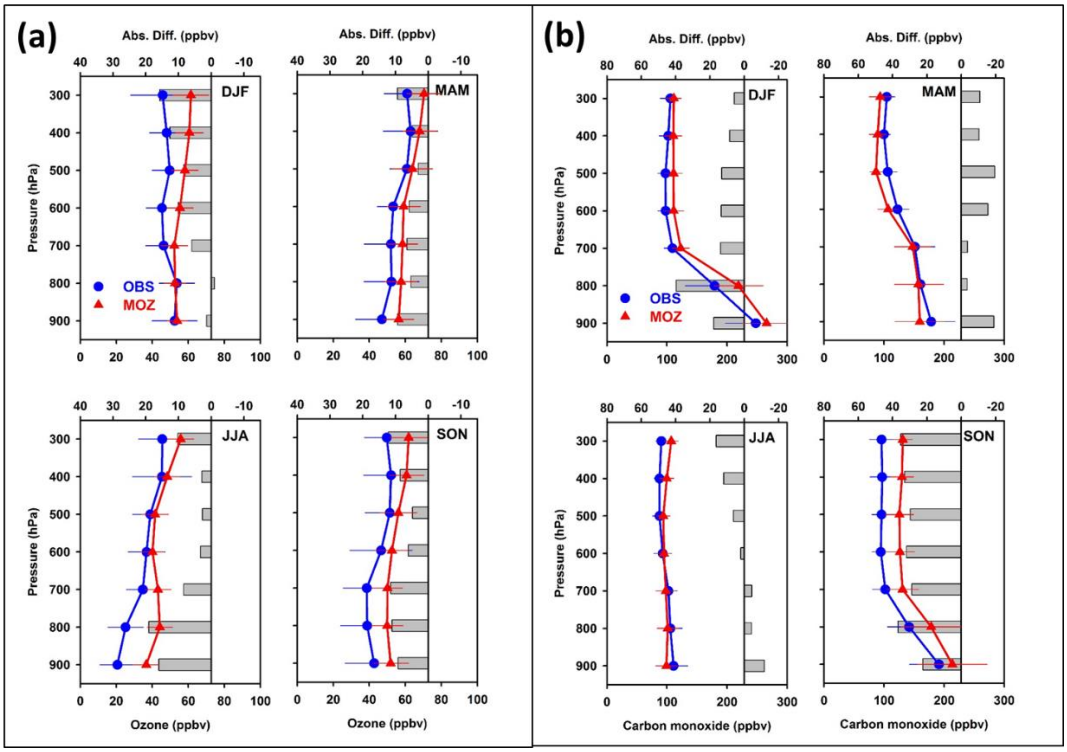

Fig. 1 a) Comparison of vertical profiles of ozone mixing ratios observed by MOZAIC aircraft (blue) and simulated (red) by MOZART-4 over Hyderabad during four seasons: summer (JJA) autumn (SON) winter (DJF) and spring (MAM). The observed O_3 profiles shown here are the seasonal variation from MOZAIC aircraft measurements during years 2007-08. Shaded grey bars show the model bias. b) Same as (a) but for CO.

3.2 Comparison with IASI measurements

The annual daily mean tropospheric column (920 - 220 hPa) of O_3 and CO from IASI and MOZART-4 are shown in Fig.2 (a) and (b) respectively. We have chosen this tropospheric column because it provides greater than 0.5 degree of freedom (the trace of the averaging kernel matrix) in the troposphere and also avoids the necessity to define a variable tropopause height (Held, 1981; S. Bethan et. al., 1996; Reichler et. al.,, 2003).

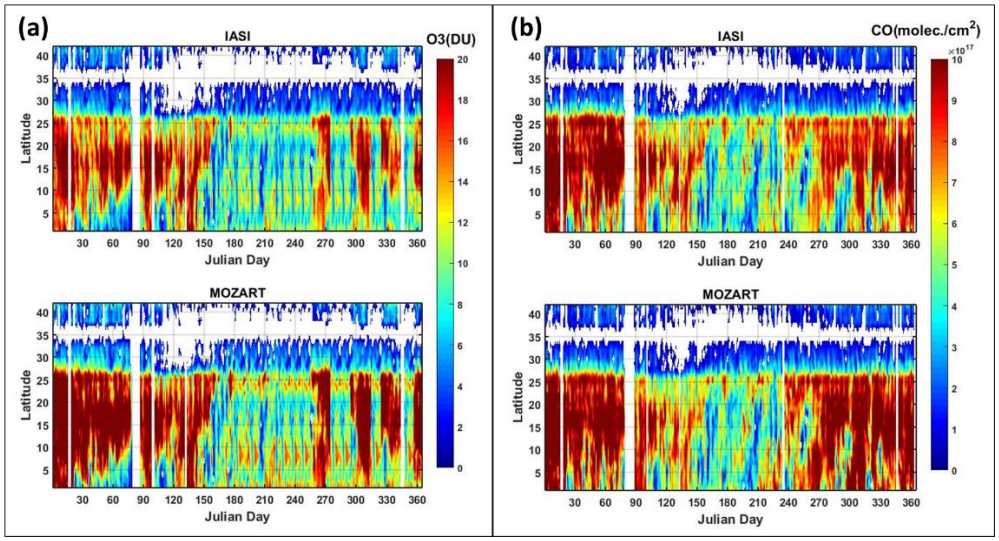

Fig. 2(a) Latitude-time plot of the zonally averaged O3 column (920 - 220 hPa) from the IASI daytime observations and their corresponding simulated by MOZART-4. The white vertical lines correspond to days with no data. (b) Same as (a) but for CO

In this study, we have analysed only IASI day time observations of the tropospheric O_3 and CO columns since the information content of IASI data has shown to be higher during the day (Clerbaux et al., 2009). The model

simulated O_3, CO column and corresponding retrieved from IASI have been compared with each other, after smoothing with IASI averaging kernel and a priory matrix. The model is able to reproduce the major features present in the satellite observations. The tropospheric column clearly shows the signature of the anthropogenic activities in O_3 tropospheric column. Highly populated regions of IGP, Arabian Sea and Bay of Bengal regions have shown high concentrations of O3 and CO column which is due to the high anthropogenic emissions over land region and the photochemical production and long range transport of the pollutants over the ocean region. The IGP is well known highly polluted/populated region. The region consists of extensive rural population. Bio - fuel is extensively used for household activities in rural areas. The emissions of O_3 precursors over Indian region are also high over these regions (not shown). The high emissions of NOx and CO are mainly attributed to the high population density.

4. Summary and Conclusions

The daily simulations of tropospheric O_3 and CO have been made using MOZART-4 during 2007-08. The model simulated O_3 and CO are evaluated against the MOZAIC and the IASI/MetOp sounder measurements. The model - simulated vertical distribution of O_3 and CO mixing ratios in the troposphere have been compared with the MOZAIC/IAGOS observations over Hyderabad. The model is being overestimated the observed O_3 concentration in terms of MB by 7.9 ppbv, 8.3 ppbv and in terms of RMSE by 13.7 ppbv , 14.5 ppbv for LT, MT respectively. The MB and RMSE are estimated for CO, 14.1 ppbv, 13.5 ppbv and 39.3 ppbv, 28.2 ppbv for LT, MT respectively. The model shows the overestimation as compared to IASI O_3 and CO column over Indian region.

References

Adams, R. M., Glyer, J. D., Johnson, S. L., & McCarl, B. a. (1989). A Reassessment of the Economic Effects of Ozone on U.S. Agriculture. *Japca*, *39*(7), 960–968. http://doi.org/10.1080/08940630.1989.10466583

Boynard, A., Clerbaux, C., Coheur, P.-F., Hurtmans, D., Turquety, S., George, M., … Meyer-Arnek, J. (2009). Measurements of total and tropospheric ozone from IASI: comparison with correlative satellite and ozonesonde observations. *Atmos. Chem. Phys. Discuss*, *9*, 10513–10548. http://doi.org/10.5194/acpd-9-10513-2009

Clerbaux, C., Boynard, a., Clarisse, L., George, M., Hadji-Lazaro, J., Herbin, H., … Coheur, P.-F. (2009). Monitoring of atmospheric composition using the thermal infrared IASI/MetOp sounder. *Atmospheric Chemistry and Physics*, *9*(16), 6041–6054. http://doi.org/10.5194/acp-9-6041-2009

Cooper, O. R., Moody, J. L., Parrish, D. D., Trainer, M., Ryerson, T. B., Holloway, J. S., … Evans, M. J. (2002). Trace gas composition of midlatitude cyclones over the western North Atlantic Ocean : A conceptual model, *107*. http://doi.org/10.1029/2001JD000901

Deeter, M. N. (2013). MOPITT (Measurements of Pollution in the Tropo- sphere) Version 6 Product User's Guide. *National Center for Atmospheric Research.*, Available at https://www2.acd.ucar.edu/sites/defau.

Emmons, L. K., Walters, S., Hess, P. G., Lamarque, J.-F., Pfister, G. G., Fillmore, D., … Kloster, S. (2010). Description and evaluation of the Model for Ozone and Related chemical Tracers, version 4 (MOZART-4). *Geoscientific Model Development*, *3*(1), 43–67. http://doi.org/10.5194/gmd-3-43-2010

Eremenko, M., Dufour, G., Foret, G., Keim, C., Orphal, J., Beekmann, M., … Flaud, J. M. (2008). Tropospheric ozone distributions over Europe during the heat wave in July 2007 observed from infrared nadir spectra recorded by IASI. *Geophysical Research Letters*, *35*(18). http://doi.org/10.1029/2008GL034803

Gauss, M. (2003). Radiative forcing in the 21st century due to ozone changes in the troposphere and the lower stratosphere. *Journal of Geophysical Research*, *108*(D9), 4292. http://doi.org/10.1029/2002JD002624

Granier, C., Bessagnet, B., Bond, T., D'Angiola, A., Denier van der Gon, H., Frost, G. J., … van Vuuren, D. P. (2011). Evolution of anthropogenic and biomass burning emissions of air pollutants at global and regional scales during the 1980–2010 period. *Climatic Change*, *109*(1–2), 163–190. http://doi.org/10.1007/s10584-011-0154-1

Held, M. (1981). On the Height of the Tropopause and the Static Stability of the Troposphere. *Journal of the Atmospheric Sciences*, *39*, 412–417.

Houghton JT, Y, D., Dj, G., M, N., Pj, V. D. L., X, D., … C, J. (2001). Climate Change 2001: The Scientific Basis. *Climate Change 2001: The Scientific Basis*, 881. http://doi.org/10.1256/004316502320517344

Jaffe, D., Mahura, A., Kelley, J., Atkins, J., Novelli, P. C., & Merrill, J. (1997). Impact of Asian emissions on the remote North Pacific atmosphere: Interpretation of CO data from Shemya, Guam, Midway and Mauna Loa. *Journal of Geophysical Research*, *102*(D23), 28627–28635. http://doi.org/10.1029/96JD02750

Kiley, C. M., Fuelberg, H. E., Palmer, P. I., Allen, D. J., Carmichael, G. R., Jacob, D. J., … Streets, D. G. (2002). An Intercomparison and Evaluation of Aircraft-Derived and Simulated CO from Seven Chemical Transport Models During the TRACE-P Experiment. *Journal of Geophysical Research*, *108*, 1–35. http://doi.org/10.1029/2002JD003089

Kim, P. S., Jacob, D. J., Liu, X., Warner, J. X., Yang, K., Chance, K., … Nedelec, P. (2013). Global ozone–CO correlations from OMI and AIRS: constraints on tropospheric ozone sources. *Atmospheric Chemistry and Physics*, *13*(18), 9321–

9335. http://doi.org/10.5194/acp-13-9321-2013

Kumar, R., Naja, M., Pfister, G. G., Barth, M. C., Wiedinmyer, C., & Brasseur, G. P. (2012). Simulations over South Asia using the Weather Research and Forecasting model with Chemistry (WRF-Chem): Chemistry evaluation and initial results. *Geoscientific Model Development*, *5*(3), 619–648. http://doi.org/10.5194/gmd-5-619-2012

Marenco, A., Thouret, V., Nédélec, P., Smit, H., Helten, M., Kley, D., … Cook, T. (1998). Measurement of ozone and water vapor by Airbus in-service aircraft: The MOZAIC airborne program, an overview. *Journal of Geophysical Research*, *103*(D19), 25631. http://doi.org/10.1029/98JD00977

Monks, P. S. (2005). Gas-phase radical chemistry in the troposphere. *Chemical Society Reviews*, *34*(5), 376–395. http://doi.org/10.1039/b307982c

Nedelec, P., Blot, R., Boulanger, D., Athier, G., Cousin, J. M., Gautron, B., … Thouret, V. (2015). Instrumentation on commercial aircraft for monitoring the atmospheric composition on a global scale: The IAGOS system, technical overview of ozone and carbon monoxide measurements. *Tellus, Series B: Chemical and Physical Meteorology*, *6*(1), 1–16. http://doi.org/10.3402/tellusb.v67.27791

Nedelec, P., Cammas, J.-P., Thouret, V., Athier, G., Cousin, J.-M., Legrand, C., … Marizy, C. (2003). An improved infrared carbon monoxide analyser for routine measurements aboard commercial Airbus aircraft: technical validation and first scientific results of the MOZAIC III programme. *Atmos. Chem. Phys.*, *3*(5), 1551–1564. http://doi.org/10.5194/acpd-3-3713-2003

Ohara, T., Akimoto, H., Kurokawa, J., Horii, N., Yamaji, K., Yan, X., & Hayasaka, T. (2007). An Asian emission inventory of anthropogenic emission sources for the period 1980–2020. *Atmospheric Chemistry and Physics Discussions*, *7*(3), 6843–6902. http://doi.org/10.5194/acpd-7-6843-2007

Reichler, T., Dameris, M., & Sausen, R. (2003). Determining the tropopause height from gridded data, *30*(20), 1–5. http://doi.org/10.1029/2003GL018240

Roy, S., Beig, G., & Jacob, D. (2008). Seasonal distribution of ozone and its precursors over the tropical Indian region using regional chemistry-transport model. *Journal of Geophysical Research*, *113*(D21), D21307. http://doi.org/10.1029/2007JD009712

S. Bethan, V. and S. J. R. (1996). A comparison of ozone and thermal tropopause heights and the impact of tropopause definition on quantifying the ozone content of the troposphere, 929–944.

Tan, Q. (2004). An evaluation of TRACE-P emission inventories from China using a regional model and chemical measurements. *Journal of Geophysical Research*, *109*(D22), D22305. http://doi.org/10.1029/2004JD005071

Thouret, V., Marenco, A., Logan, J. A., Nédélec, P., & Grouhel, C. (1998). Comparisons of ozone measurements from the MOZAIC airborne program and the ozone sounding network at eight locations. *Journal of Geophysical Research: Atmospheres*, *103*(D19), 25695–25720. http://doi.org/10.1029/98JD02243

Ukpebor, E. E., Ukpebor, J. E., Eromomene, F., Odiase, J. I., & Okoro, D. (2010). Spatial and Diurnal Variations of Carbon Monoxide (CO) Pollution from Motor Vehicles in an Urban Centre, *19*(4), 817–823.

Venkataraman, C., Habib, G., Kadamba, D., Shrivastava, M., Leon, J.-F., Crouzille, B., … Streets, D. G. (2006). Emissions from open biomass burning in India: Integrating the inventory approach with high-resolution Moderate Resolution Imaging Spectroradiometer (MODIS) active-fire and land cover data. *Global Biogeochemical Cycles*, *20*(2), n/a-n/a. http://doi.org/10.1029/2005GB002547

Wang, T. (2002). and indications of biomass burning observed at a rural site in eastern China. *Journal of Geophysical Research*, *107*(D12), 1–10. http://doi.org/10.1029/2001JD000724

Wang, T., Wong, H. L. A., Tang, J., Ding, A., Wu, W. S., & Zhang, X. C. (2006). On the origin of surface ozone and reactive nitrogen observed at a remote mountain site in the northeastern Qinghai-Tibetan Plateau, western China. *Journal of Geophysical Research Atmospheres*, *111*(8), 1–15. http://doi.org/10.1029/2005JD006527

Wigley, T. M. L., Smith, S. J., & Prather, M. J. (2002). Radiative forcing due to reactive gas emissions. *Journal of Climate*, *15*(18), 2690–2696. http://doi.org/10.1175/1520-0442(2002)015<2690:RFDTRG>2.0.CO;2

Xiao, Y., Jacob, D. J., & Turquety, S. (2007). Atmospheric acetylene and its relationship with CO as an indicator of air mass age. *Journal of Geophysical Research*, *112*(D12), D12305. http://doi.org/10.1029/2006JD008268

Yarragunta, Y., Srivastava, S., & Mitra, D. (2017). Validation of lower tropospheric carbon monoxide inferred from MOZART model simulation over India. *Atmospheric Research*, *184*, 35–47. http://doi.org/10.1016/j.atmosres.2016.09.010

Yashiro, H., Sugawara, S., Sudo, K., Aoki, S., & Nakazawa, T. (2009). Temporal and spatial variations of carbon monoxide over the western part of the Pacific Ocean. *Journal of Geophysical Research*, *114*(D8), D08305. http://doi.org/10.1029/2008JD010876